10

Spectral Features of the 1.72 eV Nickel-Based Emission Center in Nitrogen-Enriched Diamond Microcrystals

© V.Yu. Osipov[1,2], I.E. Kaliya[2], F.M. Shakhov[1], K.V. Bogdanov[2], A.V. Baranov[2]

[1] Ioffe Institute, St. Petersburg, Russia
[2] ITMO University, St. Petersburg, Russia

e-mail: osipov@mail.ioffe.ru

Received November 27, 2025
Revised November 27, 2025
Accepted December 03, 2025

Luminescence spectra of diamond microcrystals, synthesized at high pressures (5 GPa) and temperatures (1650 °C) using a nickel catalyst via spontaneous crystallization, were investigated. The nickel-related 1.72 eV emission center exhibits a complex spectral structure, including splitting of the 1.72 eV zero-phonon line and replicas arising from local phonon modes, with all spectral lines are broadened. This broadening arises from high concentrations of nitrogen impurities and other defects both point and collective incorporated into the diamond lattice. The temperature dependences of the optical center's emission-line parameters were also determined.

Keywords: synthetic diamond, nickel catalyst, covalent lattice, nickel-nitrogen complexes, optical centers, luminescence, spectral multiplets.

DOI: 10.61011/EOS.2026.02.63464.4247-25

Introduction

Synthetic diamond crystals and microcrystals grown under conditions of high pressures and high temperatures are of particular interest for the construction of advanced devices for modern photonics, devices for transmitting and optical data processing, as well as various sensors [1,2]. This is mainly due to the unprecedented variety of optical centers with unique characteristics formed in diamond crystals [3]. The most well-known emission optical centers in diamond include nitrogen-vacancy centers (NV^- and NVN), silicon-vacancy centers (SiV), germanium-vacancy centers (GeV), substitutional nickel Ni_s^+ (883 nm), a tungsten atom substituting for carbon, and many others [4–6]. The overwhelming majority of optical (and paramagnetic) centers in diamonds were well known even before the early 2000-s [7–12]. Moreover, it is the impurity nickel and its combinations in the crystal lattice with other heteroatoms or defects, such as nitrogen, vacancies and elemental hydrogen, that led to the appearance of a large group of optical centers that have been actively studied by researchers since the early 2000s [13–15]. The interest in the latter is due to optical emission beyond the visible spectral range (700−900 nm) and relative stability of such centers. In this paper, we investigate diamond crystals produced using a nickel catalyst by spontaneous crystallization (without the use of a nitrogen getter and the introduction of crystallization centers) under high pressure and high temperature conditions. The use of a nickel catalyst and the absence of a nitrogen getter result in the presence of nickel impurities in amounts of up to 10 ppm in the diamond matrix, the prevalence of nitrogen impurities (up to ∼ 290 ppm) and the appearance of complexes of the composition NiN_x in the covalent lattice of diamond. In this case, nickel enters the growing diamond lattice from the melt-catalyst material, and nitrogen from the air atmosphere. The use of nickel as a metal catalyst, leading to the formation of complex nickel-based optical centers in a growing diamond matrix, has been known for quite some time. Many of these centers with characteristic spectral signatures have been previously successfully identified [3].

Optical emission centers of the NiN_x composition were recently considered by us in [16]. In this paper, we consider an optical emission center with a complex spectral signature in the form of a sextet in the range of 695−770 nm.

Samples and methods

Sample preparation

Microcrystalline diamonds were synthesized under high pressure (5 GPa) and high temperature (1650 °C) in quasi-equilibrium conditions according to the method described in [17], using a nickel catalyst. The synthesis time of diamond crystallites was 90 s. A nickel-graphite mixture was used as a charge for synthesis. To prepare the mixture, a commercial nickel electrolytic powder of the grade PNE-1 (GOST 9722-97) and a graphite electrode powder of grade EG15 (for the manufacture of electrodes) of commercial quality with ash content of less than 0.05 wt%, produced according to the Russian standards, were used. The size of graphite particles was 315−400 μm, and the size of nickel particles did not exceed 71 μm. The prepared mixture of graphite (50 wt%) and nickel (50 wt%) powders was loaded into the central part of the toroidal high-pressure chamber. The volume fraction of nickel in the mixture was about 10%. A metal getter for nitrogen binding was

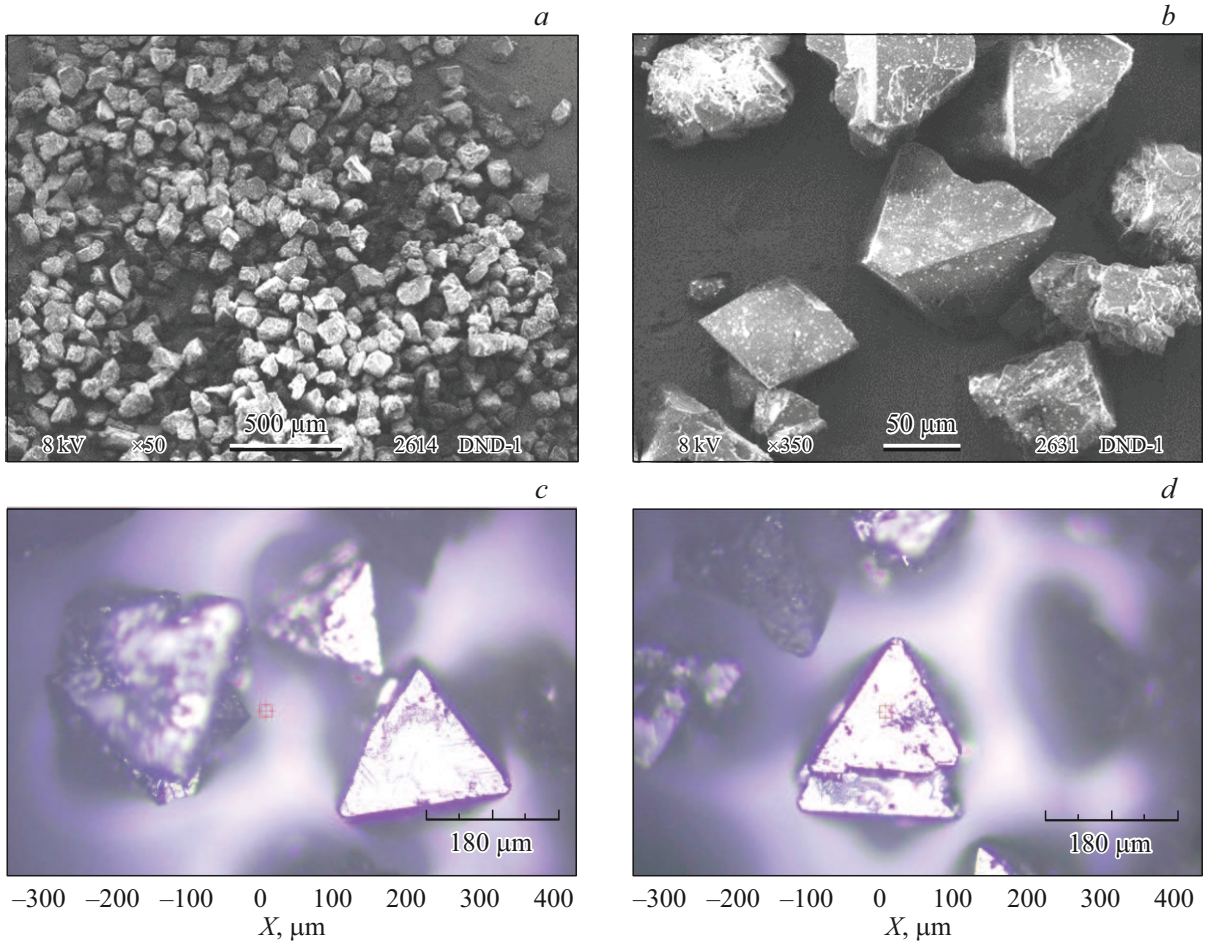

Figure 1. SEM images of microcrystals *MD*1, obtained at magnifications of 50× (*a*), 350× (*b*) and an electron beam accelerating voltage of 8 kV, together with optical images of the studied particles (*c,d*). Scale: *a* — 500 μm, *b* — 50 μm, *c,d* — 180 μm. Some individual microcrystals with characteristic facets and ribs are clearly visible in panels (*b,c,d*).

not added to the charge in order to obtain crystals with an increased nitrogen content. It should be noted that the type of synthesis used (spontaneous crystallization) did not include the introduction of micron-sized diamond seeds, i.e. crystallization centers, into the charge. During spontaneous crystallization without the use of diamond seeds, the average size of the grown crystallites turns out to be larger than with the use of seeds, and is determined mainly only by the size of the graphite particles in the charge. At a temperature of 1650 °C and a pressure of 5 GPa, nickel melts and dissolves carbon in itself. During the synthesis process, graphite gradually dissolves in molten nickel and is released from it gradually in portions in the form of diamond crystallites. Due to the continuous mass transfer of carbon material through molten nickel, the resulting microcrystals are enriched with nickel. After completion of the synthesis, diamond microcrystals were isolated from the sinter by primary grinding, etching of metallic nickel and non-diamond phase in hot acids, and rinsing in boiling water. The resulting microcrystalline diamond powder was then fractionated using an 125 μm sieve. The obtained microcrystals (fraction 125^{+} μm) were given the name *MD*1.

Elemental analysis, by X-ray fluorescence spectroscopy showed that the synthesized microcrystals contain nickel (1033 ppm), copper (283 ppm) and zirconium (1.8 ppm). The high nickel content in the material is due to its use as a metal catalyst in the synthesis of diamond, and according to X-ray diffraction data, nickel is present in the diamond lattice in the form of cubic nickel nanoparticles up to 14 nm in size. According to static magnetometry data carried out at room temperature, the concentration of superparamagnetic nickel nanoparticles in the diamond matrix is $1.45 \cdot 10^{16}$ cm^{-3}. Each nanoparticle, carrying a magnetic moment of $\sim 12\,500\,\mu_B$, contains on average about $\sim 20\,800$ nickel atoms, and the total content of metallic nickel in the diamond lattice is equal to 1720 ppm (accuracy of $\pm 2.5\%$) [18]. This estimate is in good agreement with the nickel content determined by elemental analysis. In addition to aggregated forms, nickel is present in the diamond lattice in the form of isolated impurities. Thus, according to electron paramagnetic resonance (EPR)

data, nickel centers Ni_s^- are present in the material in the charge state -1 in the positions substituting carbon atoms. The number of such centers, estimated from the intensity of the low-temperature ($T = 90$ K) EPR signal with a g-factor of $g = 2.0319$, is about 9.8 ppm. The content of impurity nitrogen in the carbon substitution positions in the crystal lattice is ~ 230 ppm according to infrared spectroscopy data (see section „Experimental results and discussion").

Morphology. Microcrystals synthesized under non-equilibrium conditions are particles of arbitrary shape, a small part of which have a faceted shape in the form of a regular octahedron. Their morphology was studied by scanning electron microscopy (SEM) using a JSM-6390 microscope (JEOL, Japan). Microcrystals selected for optical studies were additionally photographed using an optical microscope. SEM images obtained at different magnifications clearly illustrate the diversity of the synthesized particles (Fig. 1, *a,b*). Particles of arbitrary shape, without faceting, are clearly visible in Fig. 1, *a,b*, and examples of single crystalline particles of size $\sim 180\,\mu$m with characteristic facets and ribs are shown in the optical images in Fig. 1, *c,d*.

Experimental methods

Infrared absorption spectra were measured using an InfraLum FT-08 Fourier transform spectrometer (Lumex, Russia), equipped with a Pike EASIDIFF^{TM} insert, in diffuse reflectance mode. The spectral resolution was 0.7 cm^{-1}. The weight of the microcrystalline sample loaded into a 0.20 cm^3 cell was about 0.2 g with a bulk density of 1.0 ± 0.1 g $\cdot$ cm^{-3}. The method of converting the recorded reflection spectra into absorption spectra, the features of the base curve and the background subtraction procedure used in the analysis of diamond powders are described in [19].

The luminescence spectra of microcrystals were preliminarily measured at room temperature using an NTEGRA-Spectra II setup (NT-MDT „Spectrum Instruments", Russia) with focusing of the exciting radiation (wavelength 633 nm) using a 100$^\times$ microlens. The exciting laser radiation was focused directly onto the surface of the diamond microcrystal selected for analysis or into its volume at some distance from the surface. Optical images of a typical $MD1$ microcrystal, obtained by focusing 633 nm or 532 nm laser radiation (for comparison) onto it, are shown in Fig. 2, *a,b*. The study of luminescence of the synthesized microcrystalline powder ($MD1$) was carried out by recording spectra on 50–60 selected microcrystals and their subsequent analysis with division into groups with characteristic spectral signatures. The luminescence spectra of certain selected microcrystals were measured in the temperature range of 78–308 K using an InVia Raman microspectrometer (Renishaw, UK) with a liquid nitrogen-cooled CCD matrix and a diffraction grating with a line count of 1800 mm^{-1}. The spectral resolution of the spectrometer was 2 cm^{-1}. For work with cryogenic

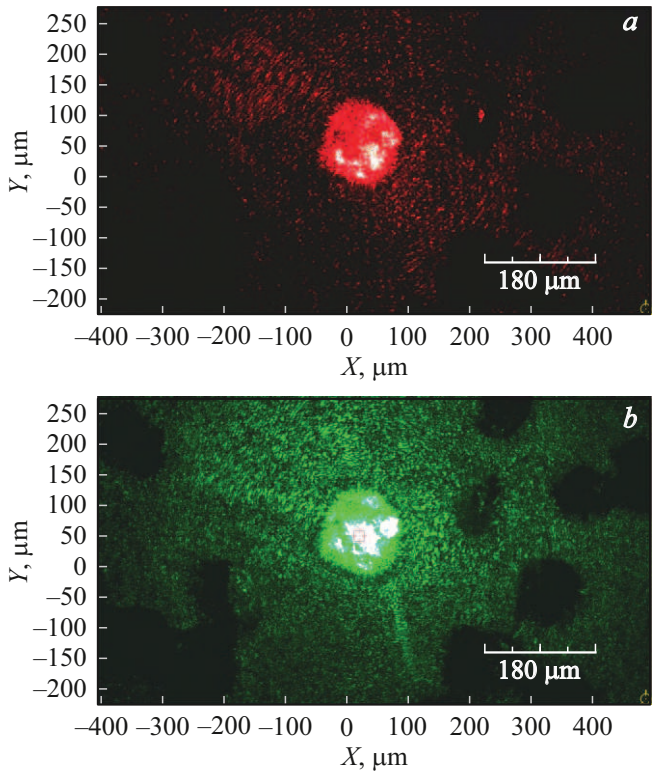

Figure 2. Optical images of a typical $MD1$ microcrystal glued to a quartz substrate, obtained by focusing laser radiation with a wavelength of 633 nm (*a*) and 532 nm (*b*) onto its surface (using an 10$^\times$ microlens). Scale: *a,b* — 180 μm.

cooling, a Linkam THMS 600 low-temperature attachment was used, and the focusing of the exciting laser radiation with a wavelength of 633 nm was carried out using an 50$^\times$ microlens with a numerical aperture of $NA = 0.50$ and a sufficient working distance to form a light spot with a diameter of $\sim 3\,\mu$m on the surface of the studied microcrystal in a low-temperature cell. To obtain the reliable data, the spectra were registered at every fixed temperature for at least 5 times. The obtained luminescence spectra were corrected taking into account the spectral sensitivity function of the spectrometer, previously determined using the radiation of a standard „black body" (THORLABS, SLS201L/M, USA). Comparison of spectra from different microcrystals was carried out, if necessary, using normalization of the luminescence intensity to the intensity of the simultaneously recorded Raman line of diamond at 1332 cm^{-1} (691 nm at excitation 633 nm) under the assumption that the intensity of the latter is proportional to the illuminated volume in the bulk of the microcrystal.

Experimental results and discussion

The infrared absorption spectrum of $MD1$ microcrystals is shown in Fig. 3. It contains the diamond's own lattice absorption band (1600–2650 cm^{-1}) and separate

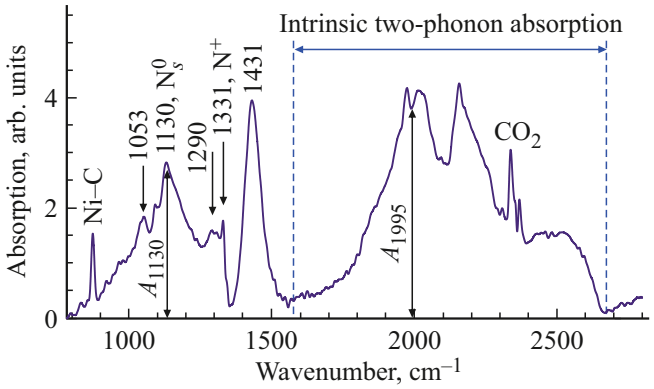

Figure 3. Infrared absorption spectrum of microcrystalline diamond powder *MD*1.

bands/lines caused by absorption at the vibrational modes of defects or impurity centers in the diamond lattice. The band at 1130 cm^{-1} is due to the isolated impurities of nitrogen (C-centers, N_s^0) in the neutral charge state in the substituting position in the diamond lattice [20], the band at 1290 cm^{-1} is due to nitrogen dimers (A-centers) in the lattice [21], peak of 1331 cm^{-1} is due to isolated impurities of nitrogen (N^+) in the charge state +1. The band at 1431 cm^{-1} is not identified, but is present only in the absorption spectra of microcrystals with a high nitrogen and nickel content, obtained using our technology. Measuring the peak intensity at 1130 cm^{-1} makes it possible to determine the concentration of C-centers in the material in units of ppm using the empirical formula [20]: N_C [ppm] $= 25\,\mu_{1995} \cdot A_{1130}/A_{1995}$, where A_{1130} and A_{1995} — intensities of absorption bands in the material for radiation with wave numbers of 1130 and 1995 cm^{-1}, μ_{1995} — optical absorption coefficient of a diamond crystal, equal to 12.3 cm^{-1} for infrared radiation with a frequency of 1995 cm^{-1}. According to this calculation, the concentration of C-centers in *MD*1 microcrystals is $\sim$ 230 ppm.

The luminescence spectra of some individual particles of microcrystals *MD*1, measured with exciting radiation at a wavelength of 633 nm, are shown in Fig. 4. These spectra contain individual lines and characteristic groups of lines from various emission centers. This makes it possible to identify groups of particles with emission centers of different types in the synthesized microcrystalline material, including those based on complexes of the NiN_x composition or isolated nickel atoms. The first group of particles (group *A*) demonstrates a characteristic unique pattern of six emission lines 700.0, 710.3, 721.2, 734.4, 749.3 and 763.1 nm from complexes of the supposed composition NiN_x and an emission line 794.7 nm from *NE*8 centers (Fig. 4, *a*). The second group of particles (group *B*) shows a high-intensity doublet line at 883 nm from Ni_s^+ or NiV^- centers (Fig. 4, *b*). The proportions of *A* and *B* particles in the microcrystalline powder are approximately $\sim$ 10% and $\sim$ 18%. Besides, the powder contains diamond microcrystals with emission at NV^- centers. Their share is about 8%. Descriptions

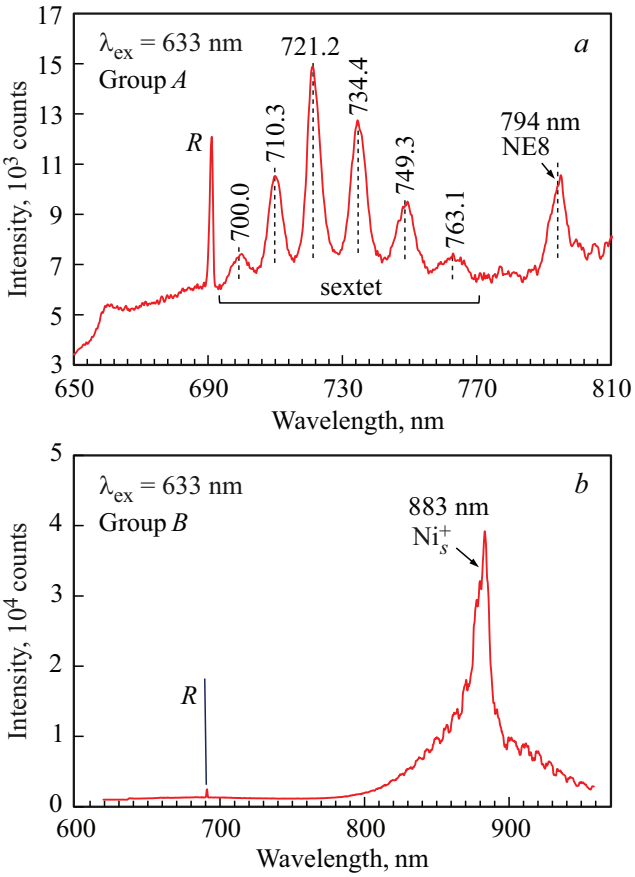

Figure 4. The luminescence spectra of diamond microcrystals selected from two groups of particles *A* and *B* (panels *a* and *b*) of the microcrystalline powder *MD*1. Optical excitation — 633 nm (oscillations in the spectral range of 830–950 nm are caused by parasitic interference at the input window of the photodetector matrix).

of other types of particles with emission in other spectral ranges can be found in the paper [22].

A sextet of six emission spectral lines is observed at room temperature with the same relative line intensities in different diamond particles,[1] which allows us to conclude that all the lines belong to the same optical center or to two morphologically related optical centers with the same environment in the crystal lattice. Besides, the quartet of lines 721.2, 734.4, 749.3 and 763.1 nm is accordingly the highly intensive zero-phonon line *L* (721.2 nm) with a set of three equidistant lines *R*1, *R*2, *R*3 (734.4, 749.3 and 763.1 nm) in the Stokes[2] area, being caused by local vibrational modes of a „heavy“ element in the luminescent complex, and emission lines 700.0 and 710.3 nm (*R*4 and *R*5)[3] in the anti-

[1] The studies were carried out on a set of 50–60 diamond particles.

[2] Here and below, terminology associated with the Stokes and anti-Stokes regions refers to the spectral zero-phonon line at 721.2 nm (1.718 eV).

[3] The zero-phonon line and its replicas in the Stokes region, associated with local phonon modes, are designated *L*, *R*1, *R*2 and *R*3, while the two emission lines lying in the short-wavelength region are designated *R*4 and *R*5.

Stokes area occur from the corresponding optical transitions in the same emission center or in the impurity complex from several heteroatoms morphologically related to the first one. Both system of emission lines correlate with each other (by relative line intensity) in all diamond particles of the A group of $MD1$ microcrystals and are not observed separately or together, but with other partial intensities. Here we assume the manifestation of local vibrational modes associated with the metal impurity atom in three spectral replicas (734.4, 749.3 and 763.1 nm) of the 721.2 nm zero-phonon line. Considering the high nickel content in the crystal lattice of $MD1$ microcrystals, these emission centers (Ni−Y) are most likely associated with impurity nickel. Here we use the notation Ni−Y, where Y is one or more agents from the immediate environment of the nickel atom, including nitrogen atoms, vacancies, or other atomic structures.

Fig. 5 shows the luminescence spectra of an individual typical microcrystal $MD1$ from the A group, recorded at several temperatures. The spectra were recalculated taking into account the spectral sensitivity function of the optical device and, after subtracting the linear background, were normalized to the intensity of the Raman line of the diamond microcrystal at 1.792 eV. It can be seen that the spectral pattern in the photon energy range 1.6−1.8 eV remains virtually unchanged with decreasing temperature. The distance between the spectral lines $R1$, $R2$, $R3$ in the Stokes region (< 1.718 eV), corresponding to the energy of local vibrational modes of „heavy“ atom in the complex, is ~ 31 meV and does not depend on the temperature in the range of 78−300 K. The intensity ratios in the spectral components (vibrational replicas) of the 1.718 eV (721.6 nm) line system remain unchanged (with an accuracy of up to 7%) with decreasing temperature. Only the relative intensities and positions of two separate spectral lines $R4$ and $R5$, located in the range of 1.732−1.8 eV, change slightly. The intensity of the broad spectral line with a centroid at 1.700 eV, shown in Fig. 5 by a dashed contour, gradually decreases with decreasing temperature to 78 K. The Huang − Rhys parameter (S) for the 1.718 eV (721.6 nm) zero-phonon line and the related Stokes system of fluorescent lines is 0.82 at $T = 288$ K. This value, for example, is slightly less than S ($S = 1.25$) for the tungsten complex in the diamond lattice [23]. The value of S remains almost unchanged (with an accuracy of up to 7−8 %) in the temperature range of 78−288 K. It means that for the emission center under study, the strength of the electron-vibrational (phonon) interaction is approximately constant in this temperature range. This feature requires further study.

In the group of particles A of diamond powder $MD1$, microcrystals with slightly different spectral characteristics and temperature dependence of the intensity of spectral components were also found. The luminescence spectra of one of these microcrystals (subgroup $A1$) are shown in Fig. 6 for three temperature values: 303, 138, and 93 K. It is seen that at a temperature of $T = 93$ K the zero-phonon line 1.718 eV (721.6 nm) is split into two spectral lines ($L1$ — 1.7191 eV and $L2$ — 1.7146 eV) with a gap

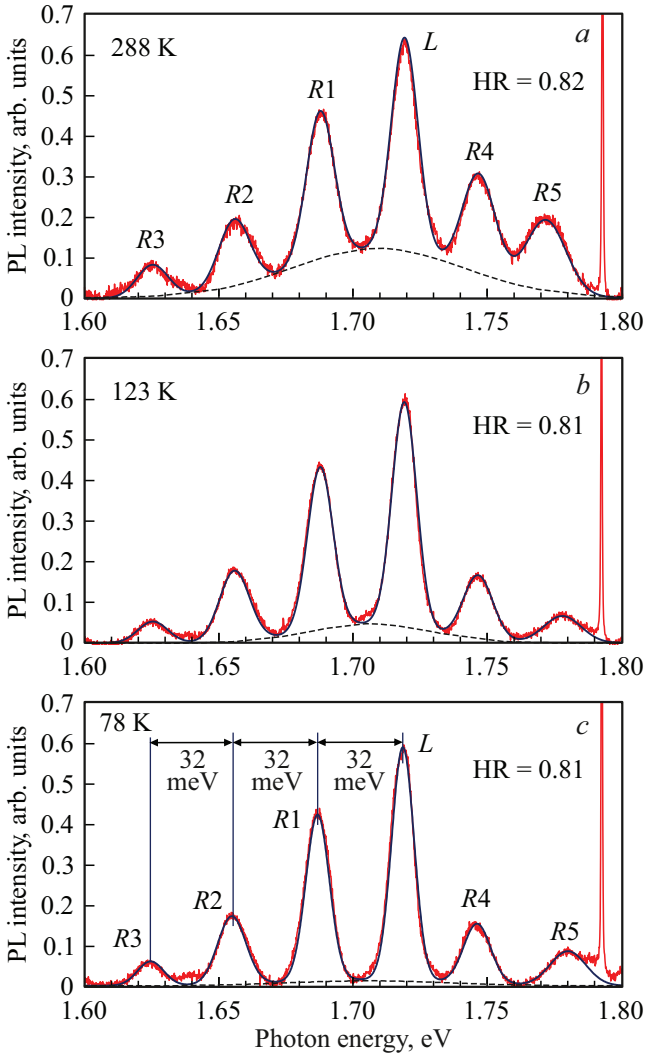

Figure 5. Luminescence spectra of an individual microcrystal selected from the group A of $MD1$ diamond powder particles, measured at temperatures of $T = 288$ K (a), 123 K (b), 78 K (c). Red line — experimental spectrum, blue line — simulated spectrum obtained using a set of Gaussian contours. Narrow line at 1.792 eV — Raman line of the diamond. Optical excitation — 633 nm. HR — Huang-Rhys parameter.

~ 4.5 meV (at 93 K), and near room temperature ($T = 303$ K) the splitting is somewhat smaller (~ 4.2 meV), but is poorly distinguishable due to the broadening of the spectral lines of the $L1/L2$ doublet. Moreover, as the temperature decreases from room temperature to $T \sim 90$ K, the lines are actually „separated“ due to the decrease in the widths of these spectral lines (Fig. 6, middle (b) and bottom (c) panels). Vibrational replicas of the 1.7146/1.7191 eV zero-phonon line also consist of components, each of which is a replica of the corresponding component of the zero-phonon line ($L1$ or $L2$), distant from it by the integer number of quanta of the local vibrational modes of the „heavy“ atom in the complex. Thus, the first two replicas in the Stokes region ($R1$ and $R2$) are well described by Lorentzian con-

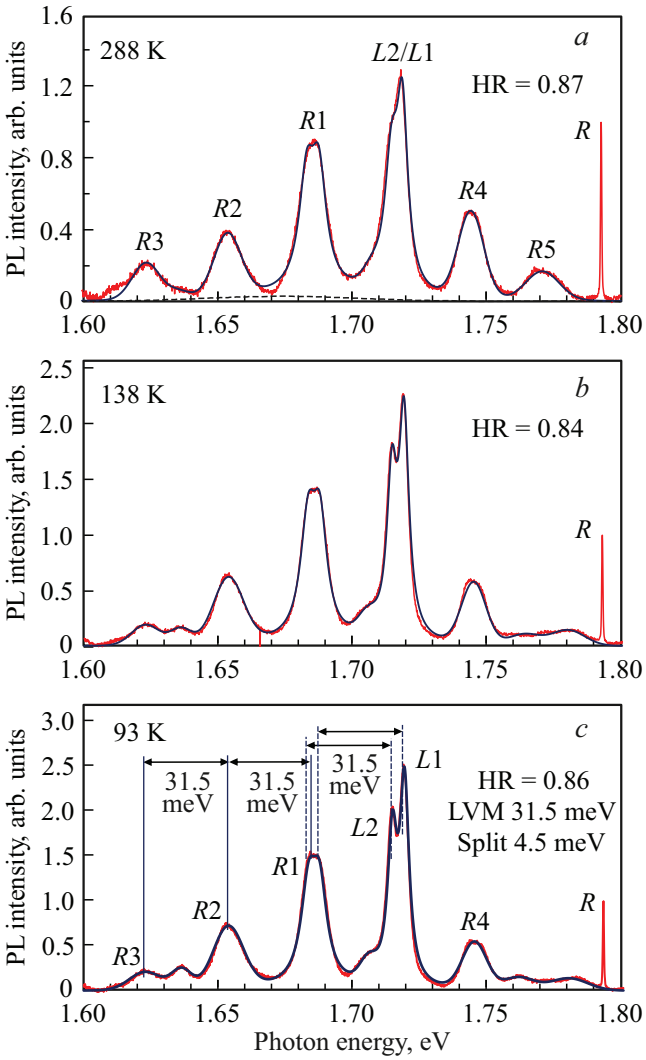

Figure 6. Luminescence spectra of an individual microcrystal selected from the $A1$ subgroup of $MD1$ diamond powder particles, measured at temperatures of $T = 303$ K (a), 138 K (b), 93 K (c). Red line — experimental spectrum, blue line — simulated spectrum obtained using a set of Lorentzian and Gaussian contours. R — Raman line of diamond. Optical excitation — 633 nm. LVM — local vibrational modes.

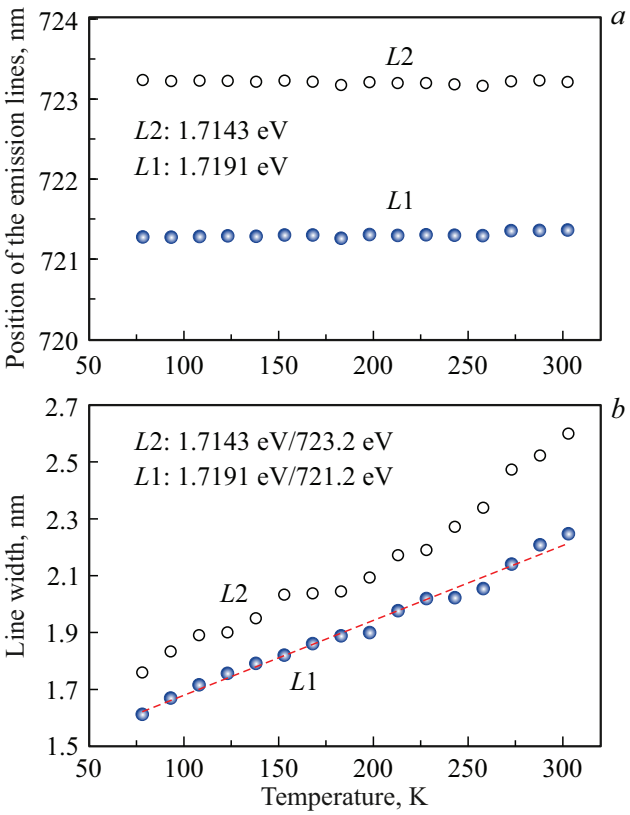

Figure 7. Temperature dependences of the wavelength (a) of the emission lines of the $L1/L2$ doublet (1.7146/1.7191 eV) and the widths (b) of the spectral components of $L1/L2$. Experimental points: dark circles — line $L1$, light circles — line $L2$.

tours with centroids spaced from the spectral components $L1$ and $L2$ (1.7191 and 1.7146 eV) by values multiples of ~ 31.5 meV. This is illustrated in Fig. 6 (bottom panel) for the luminescence spectrum obtained at a temperature of 93 K. Huang–Rhys parameter for the two-component zero-phonon line 1.7146/1.7191 eV (723.11/721.22 nm) and the corresponding Stokes system of the lines related to the spectrum of the particle from the subgroup $A1$ is approximately ~ 0.86 at $T = 93$ K and ~ 0.87 at $T = 303$ K. The temperature dependence of the position of the maxima of the spectral lines $L1$ and $L2$ is shown in Fig. 7, a. In the temperature range of 78–300 K the lines retain their position on the spectra (with an accuracy of up to ± 0.06 nm). As temperature drops from 300 down to 78 K the lines narrow approximately ~ 1.5 times (Fig. 7, b), and the intensity of both spectral components $L1/L2$ increases approximately twofold. The specified property can be useful for the tasks of non-contact local thermometry of micro-objects located in high-pressure chambers in the temperature range of 50–300 K.

A system of the zero-phonon line ~ 720 nm with replicas at ~ 736 and ~ 750 nm, due to ~ 36 meV local phonon modes, was first described by Osvet et. al in [24] using 710 nm excitation. The authors observed such a system of lines in Ni-containing synthetic diamonds (the concentration of nickel atoms 10^{18} cm^{-3}), irradiated with high-energy electrons with a dose of 10^{18} e/cm^2 and annealed at 900 °C. At temperatures of 50–100 K the zero-phonon line was split into two with a gap of about 4.7 meV, and at room temperature the splitting was not pronounced.

Subsequently, such a system of a double zero-phonon line of 720.7/722.7 nm with replicas at 734.1/736.2 and 745.2/747.9 nm was recorded in detail and described in the paper by Eliseev et al. in [25] using excitation from a helium-neon laser. The refined energy of local phonon modes was 31 meV, and the splitting of the zero-phonon line was 4.7 meV. Moreover, the same symmetrical system of vibronic lines was observed in the studied

synthetic diamonds in the anti-Stokes region (relative to the 720.7/722.7 nm line) in the luminescence excitation spectra.

The authors of both papers [21,25] associated the system of lines they observed with Ni-containing emission centers. In [25] the 1.718 eV system of lines marked with a label *NE*4[4] was assigned to the center representing the nickel atom located in the middle of divacancy $(C_3VNiVC_3)^-$. However, relatively recently, the authors of the paper [26] theoretically demonstrated that all the spectral features of the 1.718 eV line system of the center *NE*4 allow us to attribute this center to another complex, namely, one consisting of one nickel atom and three nitrogen atoms in the neutral charge state $Ni_s(N_s)_3^0$. Such assignment was made taking into account all the experimentally recorded parameters reproduced by the theory: the energy of the main optical transition, the splitting of the optically excited state, the energy of local phonon modes [26].

The 1.72 eV line system described in the literature is in good agreement with the 1.718 eV (721.6 nm) line system observed by us and the replicas from local vibrational modes with energy ~ 31 meV present in it. It is revealing that in our case for the microcrystals of the subgroup *A*1 the ~ 4.5 meV splitting is also registered, both for the 1.718 eV zero-phonon line and for its first two replicas related to the local vibrational modes. In our case, however, for the prevailing number of the microcrystals in the group *A* all spectral lines of the system 1.718 eV (721.6 nm) in the Stokes region are substantially broadened, the zero-phonon line of 1.718 eV do not demonstrate the splitting (up to the temperature of 78 K), and Huang–Rhys parameter does not depend on the temperature in the range of 78–300 K.

Thus, with the rapid (up to 90 s) synthesis of diamond microcrystals by the method of spontaneous crystallization without the use of nucleation centers, microcrystals with optical centers *NE*4 and broad emission lines are obtained. The broad emission lines of the 1.718 eV system are possibly partly due to the high concentration of centers in the diamond lattice and their diverse local environment, consisting of impurity nitrogen atoms and vacancies in different quantities. A possible reason for the inhomogeneous broadening of spectral lines in connection with the presence of aggregated (or cluster) forms of impurity nitrogen in diamond was previously mentioned in the paper by Osvet and Sildos [27]. Inhomogeneous distribution of the main donor and acceptor impurities (nitrogen and nickel) in the lattice present in different charge states should also result in the spatial fluctuations of the electrostatic potential inside the lattice. All these factors lead to fluctuations in the energy levels of the ground and excited states of the optical 1.718 eV center.

The features of the progressive splitting of the zero-phonon line of the 1.718 eV center with temperature decrease make this center attractive for use in local thermometry problems (in the range of 70–300 K and below) in high-pressure cells in studies of the properties of solids.

[4] The label *NE*4 was introduced into the nomenclature of diamond paramagnetic centers to denote nickel-containing centers that have specific signatures in electron paramagnetic resonance spectra and luminescence spectra.

Conclusion

1. Using the high-pressure, high-temperature method and a nickel catalyst, diamond microcrystals with nickel-based emission centers were synthesized. The growth of microcrystals occurs by the mechanism of spontaneous crystallization in a time of ~ 90 s.

2. In the synthesized crystals the emission centers are found with the 1.718 eV system of spectral lines including the zero-phonon line-doublet 1.7146/1.7191 eV (splitting ~ 4.5 meV at $T = 93$ K) and replicas of local phonon modes with energy of 31.5 meV distant from it.

3. Strong broadening of emission lines of 1.718 eV (*NE*4) of the optical center is related to the high content of impurity nitrogen and nickel in the microcrystals, and, including impurities in the aggregated forms.

4. In addition to the 1.718 eV (*NE*4) system of emission lines of the center, two emission lines of 1.7446 and 1.7712 eV were detected in the anti-Stokes region (for photon energies of > 1.72 eV), located at 25.5 and 52 meV relative to the zero-phonon line of 1.7191 eV. Together with the 1.7146/1.7191 eV line system, they form a unique spectral signature (sextet), which is characteristic of the grown microcrystals.

Acknowledgments

V.Yu. Osipov thanks the staff of the Laboratory of Physics of Cluster Structures at the Ioffe Institute for their assistance in using the laboratory equipment.

Information on the authors contribution

V.Yu. Osipov — formulation of the problem and conducting optical measurements at room temperature, processing and analysis of spectra, structural analysis, writing the article, I.E. Kaliya — study of luminescence and Raman scattering at low temperatures, processing of spectra, K.V. Bogdanov — study of luminescence and Raman scattering, analysis of spectra, F.M. Shakhov — synthesis of samples and their primary chemical treatment, elemental analysis, structural analysis, A.V. Baranov — analysis of optical research data, development of the concept and editing of the manuscript.

Funding

This research was supported by the Russian Science Foundation (agreement 25-15-00068).

Conflict of interest

The authors declare that they have no conflict of interest within the scope of the study presented in this article.

References

[1] T. Gaebel, I. Popa, A. Gruber, M. Domhan, F. Jelezko, J. Wrachtrup. New J. Phys., **6**, 98 (2004). DOI: 10.1088/1367-2630/6/1/098

[2] I. Aharonovich, E. Neu. Adv. Opt. Mater., **2** (10), 911 (2014). DOI: 10.1002/adom.201400189

[3] A.M. Zaitsev. *Optical Properties of Diamond: A Data Handbook, Springer-Verlag,* Berlin, Heidelberg, 2001. 502 p. DOI: 10.1007/978-3-662-04548-0

[4] M.W. Doherty, N.B. Manson, P. Delaney, F. Jelezko, J. Wrachtrup, L.C. Hollenberg. Phys. Rep., **528** (1), 1–45 (2013). DOI: 10.1016/j.physrep.2013.02.001

[5] C. Bradac, W. Gao, J. Forneris, M.E. Trusheim, I. Aharonovich. Nat. Commun., **10** (1), 5625 (2019). DOI: 10.1038/s41467-019-13332-w

[6] A.I. Shames, A. Dalis, A.D. Greentree, B.C. Gibson, H. Abe, T. Ohshima, O. Shenderova, A. Zaitsev, P. Reineck. Adv. Opt. Mater., **8** (23), 2001047 (2020). DOI: 10.1002/adom.202001047

[7] J. Loubser, J. van Wyk. Rep. Prog. Phys., **41** (8), 1201 (1978). DOI: 10.1088/0034-4885/41/8/002

[8] V. Nadolinny, A. Yelisseyev. Diam. Relat. Mater., **3** (9), 1196 (1994). DOI: 10.1016/0925-9635(94)90168-6

[9] J. Isoya, H. Kanda, J.R. Norris, J. Tang, M.K. Bowman. Phys. Rev. B, **41**, 3905 (1990). DOI: 10.1103/PhysRevB.41.3905

[10] J. Isoya, H. Kanda, Y. Uchida. Phys. Rev. B, **42**, 9843 (1990). DOI: 10.1103/PhysRevB.42.9843

[11] A.T. Collins. Diam. Relat. Mater., **9**, 417 (2000). DOI: 10.1016/S0925-9635(99)00314-3

[12] H. Kanda, K. Watanabe. Diam. Relat. Mater., **8**, 1463 (1999). DOI: 10.1016/S0925-9635(99)00070-9

[13] R.N. Pereira, A.J. Neves, W. Gehlhoff, N.A. Sobolev, L. Rino, H. Kanda. Diam. Relat. Mater., **11**, 623 (2002). DOI: 10.1016/S0925-9635(01)00578-7

[14] L. Chen, W. Shen, C. Fang, Y. Zhang, P. Mu, G. Zhou, Q. Wang, X. Jia. Cryst. Growth Des., **20** (5), 3257 (2020). DOI: 10.1021/acs.cgd.0c00080

[15] N.S. Kurochkin, V.M. Korshunov, A.V. Gritsienko, V.V. Sychev, I.V. Taydakov. Opt. Mater., 117262 (2025). DOI: 10.1016/j.optmat.2025.117262

[16] I.E. Kaliya, V.Y. Osipov, F.M. Shakhov, K. Takai, K.V. Bogdanov, A.V. Baranov. Carbon, **219**, 118839 (2024). DOI: 10.1016/j.carbon.2024.118839

[17] F.M. Shakhov, V.Yu. Osipov, A.A. Krasilin, K. Iizuka, R. Oshima. J. Solid State Chem., **307**, 122804 (2022). DOI: 10.1016/j.jssc.2021.122804

[18] F.M. Shakhov, R. Oshima, V.V. Popov. J. Phys. Chem. Sol. **185**, 111770 (2024). DOI: 10.1016/j.jpcs.2023.111770

[19] F.M. Shakhov, I.A. Ruchkin, K.S. Prilezhaev, A.M. Abyzov. Diam. Relat. Mater., **161**, 113074 (2026). DOI: 10.1016/j.diamond.2025.113074

[20] R.M. Chrenko, H.M. Strong, R.E. Tuft. Philos. Mag., **23** (182), 313–318 (1971). DOI: 10.1080/14786437108216387

[21] I. Kiflawi, A.E. Mayer, P.M. Spear, J.A. Van Wyk, G.S. Woods. Philos. Mag. B, **69** (6), 1141–1147 (1994). DOI: 10.1080/01418639408240184.

[22] V.Yu. Osipov, F.M. Shakhov, A.D. Trofimuk, K. Takai. Mend. Comm., **35** (4), 379–382 (2025). DOI: 10.71267/mencom.7649

[23] K.V. Bogdanov, I.E. Kaliya, M.A. Baranov, S.A. Grudinkin, N.A. Feoktistov, V.G. Golubev, V.Yu. Davydov, A.N. Smirnov, A.V. Baranov. Materials, **15** (23), 8510 (2022). DOI: 10.3390/ma15238510

[24] A. Osvet, A.P. Yelisseyev, B.N. Feigelson, N.A. Mironova, I. Sildos. Radiat. Eff. Defects S., **146** (1–4), 339–348 (1998). DOI: 10.1080/10420159808220306

[25] A. Yelisseyev, S. Lawson, I. Sildos, A. Osvet, V. Nadolinny, B. Feigelson, J.M. Baker, M. Newton, O. Yuryeva. Diam. Relat. Mater., **12**, 2147–2168 (2003). DOI: 10.1016/S0925-9635(03)00256-5

[26] G. Thiering, A. Gali. Phys. Rev. Research, **3**, 043052 (2021). DOI: 10.1103/PhysRevResearch.3.043052

[27] A. Osvet, I. Sildos. Radiat. Eff. Defects S., **136** (1–4), 227–231 (1995). DOI: 10.1080/10420159508218825

Translated by M.Verenikina